

NUMERICAL STUDIES OF FLUID-ROCK INTERACTIONS IN ENHANCED GEOTHERMAL SYSTEMS (EGS) WITH CO₂ AS WORKING FLUID

Tianfu Xu, Karsten Pruess and John Apps

Earth Sciences Division
Lawrence Berkeley National Laboratory
One Cyclotron Road
Berkeley, California, 94506, USA
E-mail: Tianfu_Xu@lbl.gov

ABSTRACT

There is growing interest in the novel concept of operating Enhanced Geothermal Systems (EGS) with CO₂ instead of water as heat transmission fluid. Initial studies have suggested that CO₂ will achieve larger rates of heat extraction, and can offer geologic storage of carbon as an ancillary benefit. Fluid-rock interactions in EGS operated with CO₂ are expected to be vastly different in zones with an aqueous phase present, as compared to the central reservoir zone with anhydrous supercritical CO₂. Our numerical simulations of chemically reactive transport show a combination of mineral dissolution and precipitation effects in the peripheral zone of the systems. These could impact reservoir growth and longevity, with important ramifications for sustaining energy recovery, for estimating CO₂ loss rates, and for figuring tradeoffs between power generation and geologic storage of CO₂.

INTRODUCTION

The U.S. Department of Energy has broadly defined Enhanced (or Engineered) Geothermal Systems (EGS) as engineered reservoirs that have been created to extract economical amounts of heat from geothermal resources of low permeability and/or porosity (MIT, 2006). The MIT report indicated that EGS could become a major supplier of primary energy for U.S. base-load generation capacity by 2050. Here we consider a novel EGS concept that would use carbon dioxide (CO₂) instead of water as heat transmission fluid, and would achieve geologic sequestration of CO₂ as an ancillary benefit (Brown, 2000).

Numerical simulations of fluid dynamics and heat transfer indicate that CO₂ is superior to water in its ability to mine heat from hot fractured rock (Pruess, 2006). Carbon dioxide also offers advantages with respect to wellbore hydraulics, in that its larger

compressibility and expansivity as compared to water would increase buoyancy forces and reduce the parasitic power consumption of the fluid circulation system. While the thermal and hydraulic aspects of a CO₂-EGS system look promising, major uncertainties remain with regard to chemical interactions between fluids and rocks.

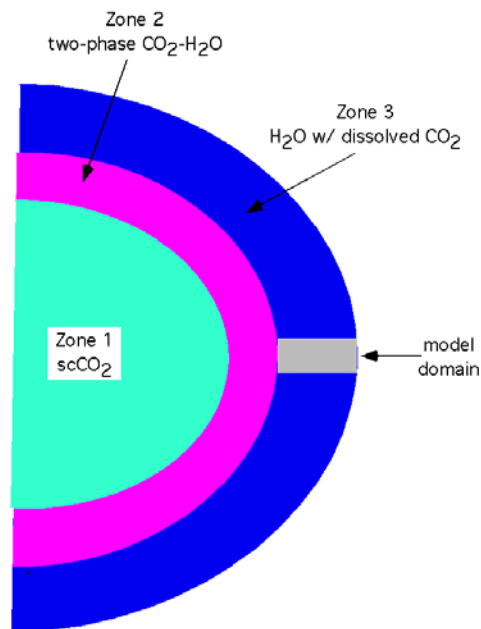


Figure 1. Schematic showing portions of the three zones with different phase compositions in an EGS operated with CO₂. The model domain studied in this paper is in the single-phase Zone 3, extending from the two-phase Zone 2 on the left to the outer boundary of the EGS on the right. "sc" stands for supercritical CO₂.

As shown in Figure 1, a fully developed EGS with CO₂ would consist of three distinct zones (Fouillac et al., 2004; Ueda et al., 2005), (1) a central zone or

“core” (Zone 1) in which all aqueous phase has been removed by dissolution into the flowing CO₂ stream, so that the reservoir fluid is a single supercritical CO₂ phase; (2) a surrounding intermediate zone (Zone 2), in which the reservoir fluid consists of a two-phase water-CO₂ mixture; and (3) an outer or peripheral zone (Zone 3), in which the reservoir fluid is a single aqueous phase with dissolved CO₂.

Geochemical processes are expected to be quite different in the three zones. The absence of water in the inner (core) zone poses unique questions, as little is presently known about the geochemistry of non-aqueous systems. The aqueous fluids initially present in an EGS reservoir would be quickly removed by immiscible displacement by the CO₂, and by dissolution (evaporation) into the flowing CO₂ stream. Continuous operation of a CO₂-EGS may produce a rather dry CO₂ stream. Research on reactions between supercritical CO₂ and rocks in the absence of water has started only recently (Regnault et al., 2005). Carbon dioxide is not an ionic solvent, which would reduce the potential for dissolution and subsequent re-precipitation of minerals, and avoid problems of scaling and formation plugging (Brown, 2000). It appears likely that prolonged exposure to supercritical CO₂ will cause dehydration reactions that would remove loosely bound water from rock minerals. Such reactions may reduce the molar volume of the minerals involved, which would increase porosity and permeability of the formations, and might promote reservoir growth (Pruess, 2006).

Rock-fluid interactions in Zones 2 and 3 would be mediated by the aqueous phase. Some information on relevant processes is available from laboratory experiments (Ueda et al., 2005), natural CO₂-bearing geothermal systems (Giolito et al., 2007), and reactive chemical transport modeling (André et al., 2007; Gherardi et al., 2007). The peripheral zone (Zone 3) of an EGS operated with CO₂ may experience a combination of mineral dissolution and precipitation effects that could impact reservoir growth and longevity. The long-term behavior of this outermost zone will be crucial for sustaining energy recovery, for estimating CO₂ loss rates, and for figuring tradeoffs between power generation and geologic storage of CO₂. We have performed reactive transport simulations to study CO₂-induced mineral alteration in the outer zone, associated changes in reservoir porosity, and sequestration of CO₂ by secondary carbonate precipitation.

PROBLEM SETUP

Geometric and Flow Conditions

Before moving into site-specific investigations, general CO₂-EGS features and issues should be explored. This can be done by abstracting site-

specific features and thereby attempt to represent characteristics that may be common to many of these systems. Basic issues are the physical and chemical changes induced by dissolved CO₂, including dissolution of primary minerals, formation of secondary minerals, CO₂ mineral trapping, and changes in reservoir porosity and permeability.

As pointed out by Gherardi et al. (2007), when interactions between CO₂-rich fluid and rocks occur under fully liquid-saturated conditions and a diffusion-controlled regime, pH will be buffered at higher values, favoring carbonate precipitation that leads to further sealing of the caprock of the CO₂ storage reservoir. Even though their simulations were performed for a low temperature of 45 °C, the peripheral zone in a higher temperature CO₂-EGS reservoir may show similar trends. In the simulations presented here, we used a one-dimensional model (Figure 1). At the left boundary of the model domain, water chemical composition was specified by equilibrating with a high CO₂ pressure and primary mineral assemblage (see below), to represent the single-aqueous-phase peripheral zone of a CO₂-EGS reservoir. The right boundary is closed for water flow and chemical transport. The 1-D linear flow model allows us to identify the geochemical parameters and controls that have the most sensitive influence on reservoir behavior. The geometric and hydrogeologic specifications of the 1-D flow problem are given in Table 1. The simulation was performed under an isothermal condition of 200 °C. Temperature and pressure at the left and right boundaries are set to be constants throughout the simulation and equal to their initial values, or 200 °C and 500 bar. Therefore, advection would occur only in response to pressure changes from dissolution and precipitation reactions.

Table 1. Geometric and hydrogeologic specifications for 1-D linear flow problem.

Geometric variables:	
Length of the column	12 m
Gridding	60 x 0.2 m
Cross-section area	1 m ²
Reservoir properties:	
Permeability	1×10 ⁻¹³ m ²
Porosity	10 %
Rock grain density	2600 kg/m ³
Rock specific heat	920 J/kg/°C
Thermal conductivity	2.51 W/m/°C
Initial and boundary conditions:	
Pressure	500 bar
Temperature	200 °C
Aqueous transport:	
Tortuosity	0.46
Aqueous diffusion coefficient	1×10 ⁻⁹ m ² /s

Mineralogical Composition and Reaction Kinetics

The present study is not intended to represent any particular site. However, data for mineralogical composition were taken from the European Hot Dry Rock research site (HDR, Soultz project), which is situated at Soultz-sous-Forêts, northern Alsace, France (Jacquot, 2000; Durst, 2002; Bächler, 2003; André et al., 2006). The Soultz reservoir is composed of altered granite blocks partly cemented by alteration products that consist essentially of clay minerals and carbonates (see Table 2). As the primary minerals initially present in the rock matrix dissolve due to CO₂ intrusion, some secondary carbonate minerals (siderite, ankerite and dawsonite) may be formed; all these minerals were included in the simulation. Mineral dissolution and precipitation are considered under kinetic constraints. A general kinetic rate expression is considered, which is based on transition state theory (Lasaga et al., 1994). The parameters used are taken from Xu et al. (2006).

Table 2. List of initial mineral volume fractions in altered granite from Soultz (Jacquot, 2000; Durst, 2002; Bächler, 2003) and potential secondary mineral phases (with zero volume fractions).

Mineral	Volume fraction in term of solid	Specific surface area A (cm ² /g)
Primary:		
Quartz	0.0409	9.8
Calcite	0.033	9.8
K-feldspar	0.139	9.8
Chlorite	0.048	108.7
Dolomite	0.008	9.8
Na-smectite	0.07469	108.7
Ca-smectite	0.02231	108.7
Pyrite	0.007	12.9
Illite	0.246	108.7
Non-reactive	0.3681	
Secondary:		
Amorphous silica (precipitation)		9.8
Siderite		9.8
Ankerite		9.8
Dawsonite		9.8

Water Chemistry

We started with a 165 °C water sample taken from Soultz Well CPK1 at 3500 m depth. Initial water chemistry in the porous medium column was obtained by equilibrating the measured water composition with their corresponding primary mineral assemblage (Table 2) at a temperature of 200

°C. The resulting initial water composition is shown in Table 3. The important boundary parameter controlling rock-fluid interactions is the aqueous concentration of CO₂. At the left boundary, we applied a water that was obtained by equilibrating the initial water with a CO₂ partial pressure of 350 bar. The resulting chemical composition of the boundary water is also given in Table 3.

Table 3. List of chemical compositions (units are mol/kg H₂O except for pH) of initial and boundary waters used in the simulation, which were derived from a Soultz Well GPK1 sample (Durst, 2002).

Water type	Initial water	Boundary water
Chemical components	Equilibrium with the minerals (200°C)	
Ca	1.705×10 ⁻¹	2.122×10 ⁻¹
Mg	5.536×10 ⁻³	6.949×10 ⁻³
Na	1.211	1.147
K	9.432×10 ⁻²	3.178×10 ⁻²
Fe	1.981×10 ⁻⁷	8.792×10 ⁻³
Cl	1.719	1.686
SiO ₂ (aq)	4.131×10 ⁻³	3.758×10 ⁻³
Total CO₂(aq)	1.724×10⁻³	1.071
SO ₄	2.391×10 ⁻³	1.990×10 ⁻³
Al	1.519×10 ⁻⁶	1.113×10 ⁻⁶
pH	5.7	4.2

Simulation Tool

The simulations employed the non-isothermal reactive geochemical transport code TOUGHREACT (Xu et al., 2006); which introduces reactive chemistry into the multiphase fluid and heat flow code TOUGH2 (Pruess, 2004). More information on the TOUGHREACT can be found at <http://www-esd.lbl.gov/TOUGHREACT/>.

Temporal changes in reservoir rock porosity and permeability due to mineral dissolution and precipitation can modify fluid flow path characteristics. This feedback between flow and chemistry is considered in our model. Changes in porosity are calculated from variations in mineral volume fractions. A simple cubic Kozeny-Carman grain model was used in the current problem

$$\frac{k}{k_0} = \left(\frac{\phi}{\phi_0} \right)^3 \left(\frac{1-\phi_0}{1-\phi} \right)^2 \quad (1)$$

where ϕ is the porosity, k is the permeability (in m²), and subscripts 0 denote initial variable values. A broad range of subsurface thermal-physical-chemical processes are considered under various

thermohydrological and geochemical conditions of pressure, temperature, water saturation, ionic strength, pH and Eh. Further details on the process capabilities of the TOUGHREACT code are given in Xu et al. (2006)

RESULTS AND DISCUSSION

The pH distribution along the column is presented in Figure 2. The initial value throughout the column is close to 6. The pH close to the left boundary has a value of 4.5, higher than at the boundary (4.2; see Table 3), which is buffered by mineral assemblage. The pH evolution is caused by both transport and reactions. Distribution of conservative tracer concentrations is presented in Figure 3, to illustrate transport contribution.

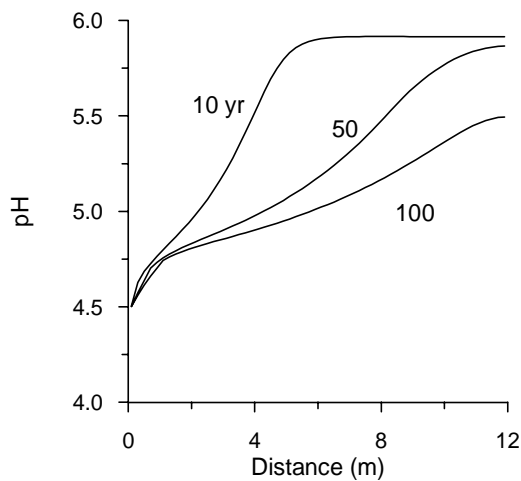


Figure 2. pH distribution at different times obtained from the 1-D problem using a Soutz mineralogy. The left of the model domain (see Figure 1) is at $x = 0$ m.

The total dissolved CO_2 concentrations, including $\text{CO}_2(\text{aq})$ and associated aqueous species such as HCO_3^- , CO_3^{2-} , CaHCO_3^+ , MgHCO_3^+ , and FeHCO_3^+ , are presented in Figure 4. The total CO_2 concentration close to the left boundary has a value of 1.2 mol/kg, which is somewhat larger than in the boundary water (in Table 3, boundary value is 1.07 mol/kg H_2O). This is because precipitation of the secondary clay minerals smectite and illite consumes H_2O (hydration) which was considered in our geochemistry model.

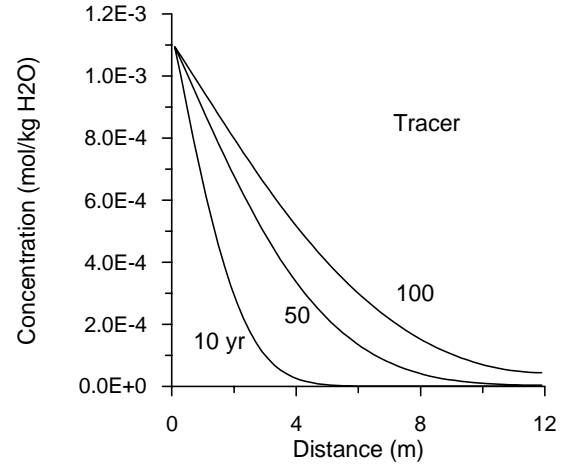


Figure 3. Concentrations of a conservative solute tracer at different times.

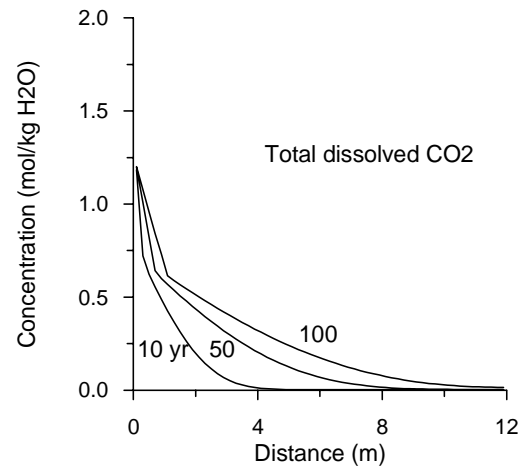


Figure 4. Distribution of total $\text{CO}_2(\text{aq})$ concentrations at different times.

The lowered pH due to the intrusion of CO_2 -rich water induces dissolution of primary minerals such as calcite, K-feldspar, and chlorite, and precipitation of secondary carbonate and clay minerals such as siderite, dolomite, smectite and illite. Consequently, porosity decreases significantly close to the left boundary (Figure 5), because (1) CO_2 -rich water adds solute mass to the rock matrix and (2) molar volumes of secondary clays are larger than those of the primary minerals. The extent of porosity change is consistent with the mineral alteration mentioned above. The porosity was reduced up to 0.094, from the initial value of 0.1.

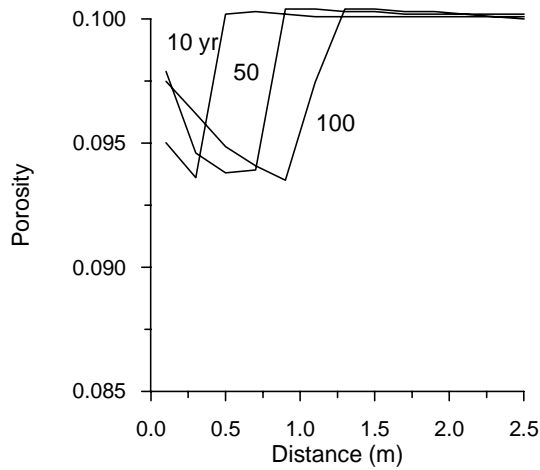


Figure 5. Profiles of porosity at different times.

Although calcite was initially present in the rocks, it generally dissolves due to the low pH. The calcite dissolution front moves with time (Figure 6). K-feldspar dissolution occurs close to the CO₂ source and gradually decreases away from it (Figure 7). As primary minerals dissolve, secondary carbonate and clay minerals are formed. Chlorite (Figure 8) dissolves and supplies Mg and Fe to induce dolomite (Figure 9) and siderite (Figure 10) precipitation.

The precipitation fronts of dolomite and siderite move with time, coinciding with the fronts of dissolution of calcite (Figure 6) and chlorite (Figure 8). Precipitation of clay minerals (smectite-Na, smectite-Ca, and illite) was observed in the simulation; only that of smectite-Na is presented in Figure 11. Precipitation of dolomite and siderite sequesters a significant amount of CO₂ (Figure 12). A maximum of about 50 kg CO₂ per m³ of medium was trapped by carbonate precipitation.

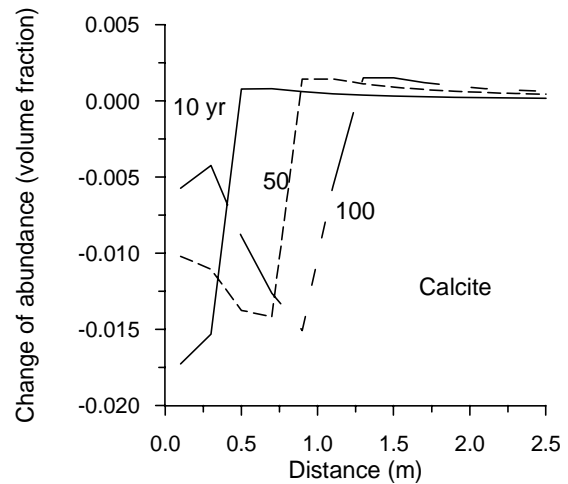


Figure 6. Changes of calcite abundance (in volume fraction in terms of porous medium; positive values indicate precipitation and negative dissolution) along the distance at different times.

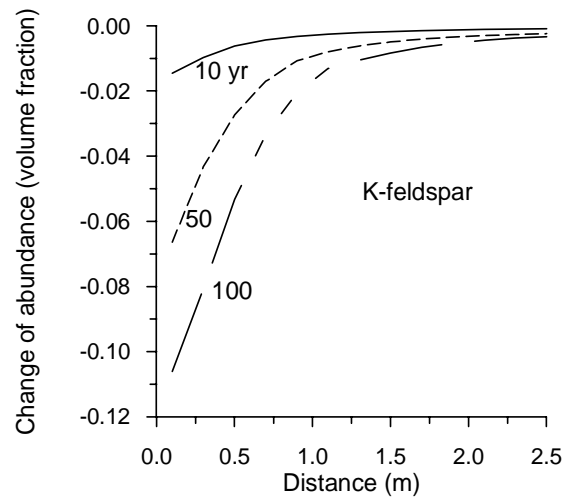


Figure 7. Changes of K-feldspar abundance along the column at different times.

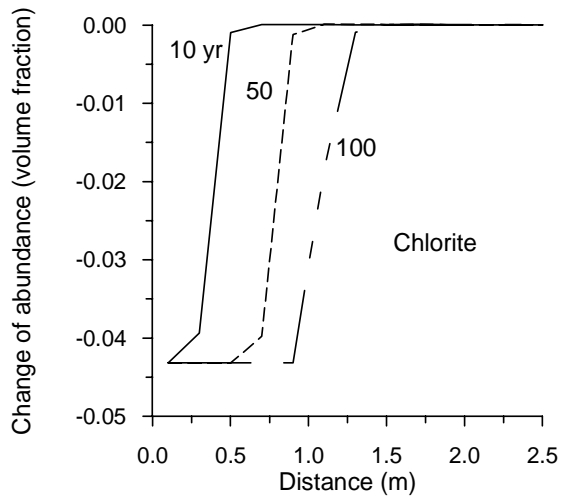


Figure 8. Changes of chlorite abundance along the column at different times.

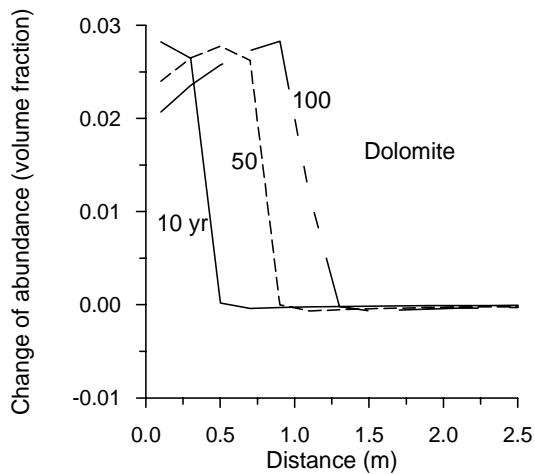


Figure 9. Changes of dolomite abundance along the column at different times.

In the previous simulation, we considered dolomite precipitation, which under field conditions tends to be kinetically inhibited. To evaluate the impact on mineral alteration, porosity change, and CO₂ mineral trapping when dolomite precipitation is disregarded, we performed an additional simulation. In this case, ankerite precipitation occurs because of Mg surplus without consumption by dolomite precipitation. Siderite precipitation still occurs, but the amount is smaller. The extent of porosity change is slightly smaller (compare Figures 5 and 13). The zone of CO₂

trapped (Figure 14) by ankerite and siderite precipitation is slightly narrower (compare Figures 12 and 14), but the maximum of CO₂ mineral trapping is similar (50 kg/m³ medium).

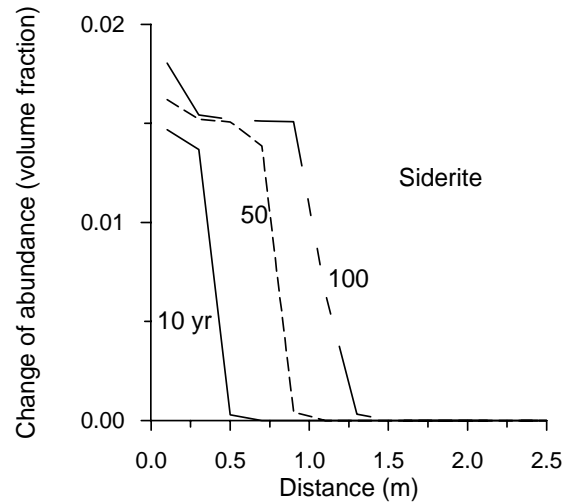


Figure 10. Changes of siderite abundance along the column at different times.

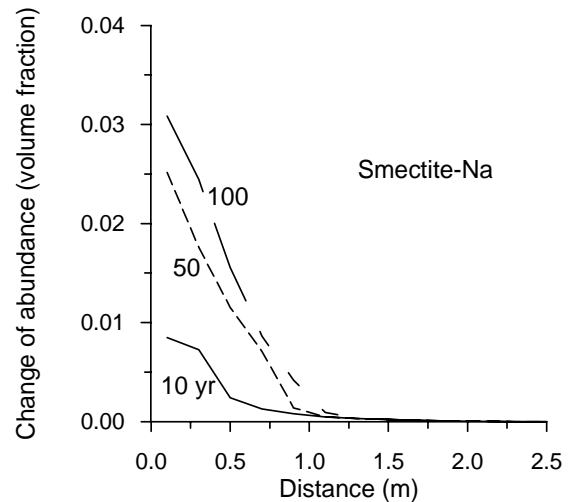


Figure 11. Changes of smectite-Na abundance along the column at different times.

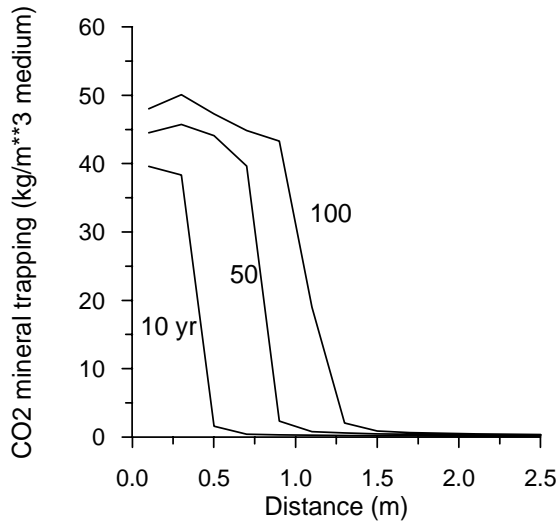


Figure 12. Cumulative amounts of CO₂ sequestered by secondary carbonate precipitation along the column at different times.

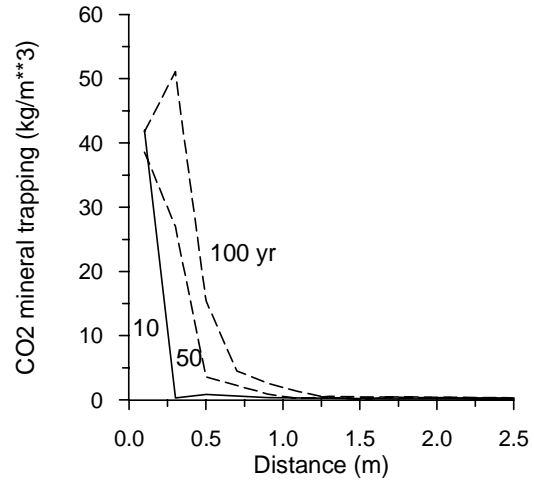


Figure 14. Cumulative amounts of CO₂ sequestered by secondary carbonate precipitation at different times obtained from the additional simulation.

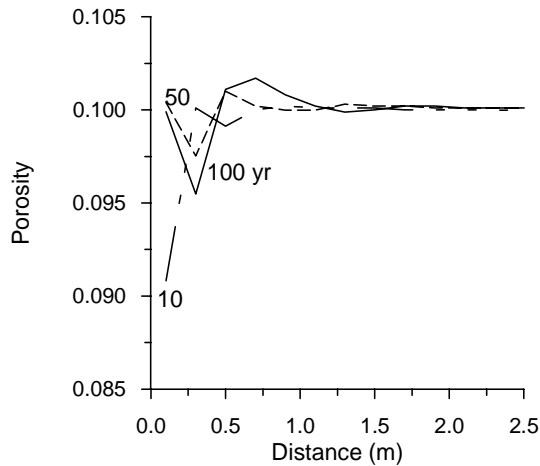


Figure 13. Distribution of porosity along the column at different times obtained from the additional simulation without considering dolomite precipitation.

CONCLUSIONS AND RECOMMENDATIONS

We have developed a one-dimensional model for the peripheral zone of a CO₂-EGS system using the mineralogical composition and water chemistry from the Soutz EGS site. Major findings from our simulation are:

- Dissolved CO₂ may diffuse to the peripheral zone of the EGS and induce dissolution of primary minerals and precipitation of secondary carbonate and clay minerals. For Soutz mineralogy, the main dissolving minerals are calcite, K-feldspar, and chlorite. Major precipitating secondary carbonates are dolomite, siderite and ankerite, and clay minerals are Na-smectite, Ca-smectite and illite.
- The transport of dissolved CO₂ and mineral alteration generally decreases porosity, which could result in the formation of a lower permeable barrier that would impact reservoir growth and longevity. Significant CO₂ could be fixed through precipitation of carbonate minerals, which can offer geologic storage of carbon as an ancillary benefit.

The time frame to form a lower permeable barrier and the fixation of CO₂ is a function of reaction kinetics of mineral dissolution and precipitation, which requires further study. The extent of porosity decrease and amount of CO₂ mineral trapping depends on the primary mineral composition.

Sensitivity studies on different rock mineralogies should be performed in the future. Using natural analogues of high-pressure CO₂ reservoirs, refinements on thermodynamic, kinetic and physical data should be useful. Reactivity between supercritical CO₂ and rock is not well understood. Experimental studies are required to quantitatively describe the reaction kinetics. Investigations on chemical changes for the entire reservoir domain should be addressed in the future.

ACKNOWLEDGEMENT

We thank Marcelo Lippmann and Guoxiang Zhang for reviews of the manuscript. This work was supported by Contractor Supporting Research (CSR) funding from Berkeley Lab under Contract No. DE-AC02-05CH11231 with the U.S. Department of Energy.

REFERENCES

André, L., Audigane, P., Azaroual, M., Menjot, A. (2007), "Numerical Modeling of Fluid-rock Chemical Interactions at the Supercritical CO₂ - liquid Interface During CO₂ Injection into a Carbonate Reservoir, the Dogger Aquifer (Paris Basin, France)," *Energy Conv. Mgmt.*, **48**, 1782-1797.

André, L., Rabemanana, V., Vuataz, F.-D. (2006), "Influence of water-rock interactions on fracture permeability of the deep reservoir at Soultz-sous-Forêts, France," *Geothermics*, **35**, 507-531.

Bächler, D. (2003), "Coupled Thermal-hydraulic-chemical Modeling at the Soultz-sous-Forêts HDR Reservoir (France)," PhD dissertation, Swiss Federal Institute of Technology, Zurich, Switzerland.

Brown, D. (2000), "A Hot Dry Rock Geothermal Energy Concept Utilizing Supercritical CO₂ Instead of Water," In: Proceedings of the Twenty-Fifth Workshop on Geothermal Reservoir Engineering, Stanford University, pp. 233-238.

Durst, D. (2002), "Geochemical Modeling of the Soultz-sous-Forêts Hot Dry Rock Test Site: Coupled Fluid-rock Interaction to Heat and Fluid Transport," PhD dissertation, Université de Neuchâtel, France.

Fouillac, C., Sanjuan, B., Gentier, S., Czernichowski-Lauriol, I. (2004). "Could Sequestration of CO₂ be Combined with the Development of Enhanced Geothermal Systems," paper presented at Third Annual Conference on Carbon Capture and Sequestration, Alexandria, VA, May 3-6.

Gherardi, F., Xu, T., Pruess, K. (2007), "Numerical Modeling of Self-limiting and Self-enhancing Caprock Alteration induced by CO₂ storage in a Depleted Gas Reservoir," *Chem. Geol.*, **244**, 103-129.

Giolito, Ch., Ruggieri, G., Gianelli, G. (2007), "Fluid Evolution in the Deep Reservoir of the Mt. Amiata Geothermal Field, Italy," Transactions, Geothermal Resources Council, **31**, 153-158.

Jacquot, E. (2000), *Modélisation Thermodynamique et Cinétique des Reactions Géochimiques Entre Fluids de Basin et Socle Cristalline*, Application au Site Experimental du Programme Européen de Recherché en Géothermie Profonde (Soultz-sous-Forêts, Bas Rhin, France), PhD dissertation, Univ. Louis Pasteur, Strasbourg, France.

Lasaga, A.C., Soler, J.M., Ganor, J., Burch, T.E., Nagy, K.L. (1994), Chemical Weathering Rate Laws and Global Geochemical Cycles, *Geochimica et Cosmochimica Acta*, **58**, 2361-2386.

MIT, (2006), "The Future of Geothermal Energy Impact of Enhanced Geothermal Systems (EGS) on the United States in the 21st Century," A Report for the U.S. Department of Energy, Massachusetts Institute of Technology.

Pruess, K. (2004), "The TOUGH Codes - A Family of Simulation Tools for Multiphase Flow and Transport Processes in Permeable Media," *Vadose Zone Journal*, **3**, 738-746.

Pruess, K (2006), "Enhanced Geothermal Systems (EGS) Using CO₂ as Working Fluid - A Novel Approach for Generating Renewable Energy With Simultaneous Sequestration of Carbon," *Geothermics*, **35**, 351-367.

Regnault, O., Lagneau, V., Catalette, H., Schneider, H. (2005), "Étude Expérimentale de la Réactivité du CO₂ Supercritique vis-à-vis de Phases Minérales pures. Implications pour la Sequestration Géologique de CO₂," *C. R. Geoscience*, **337**, 1331-1339.

Ueda, A., Kato, K., Ohsumi, T., Yajima, T., Ito, H., Kaieda, H., Meycalf, R., Takase, H. (2005), "Experimental Studies of CO₂-rock Interaction at Elevated Temperatures Under Hydrothermal Conditions," *Geochem. J.*, **39**, 417-425.

Xu, T., Sonnenthal, E.L., Spycher, N., Pruess, K. (2006), "TOUGHREACT: A Simulation Program for Non-isothermal Multiphase Reactive Geochemical Transport in Variably Saturated Geologic Media," *Computer & Geosciences*, **32**, 145-165.